

V.A.Sadovnikova

On the relation between the long-wave instability and the pion condensation in nuclear matter

Abstract

The solutions to the zero-sound frequency equation and pion dispersion equation are considered for the different values of the parameters of the effective particle-hole interaction. The branches of solutions, responsible for the long-wave instability (Pomeranchuk,[1]) of the nuclear matter $\omega_P(k)$ are presented for the both equations. It is shown that in the pion dispersion equation the solutions $\omega_P(k)$ result in the instability not only for values of the spin-isospin constant $g' \leq -1/2$, violating stability criteria, but for all $g' < g'_p$ ($|g'_p| \ll 1$ and $g'_p < 0$). At $g' > g'_p$ the branches $\omega_P(k)$ turn into the solutions responsible for pion condensation.

Introduction

In this paper the various excitations in symmetric nuclear matter are investigated. The nuclear matter is considered as a normal Fermi liquid [2, 3]. The quasiparticle-quasihole interaction is taken in the form [4, 5]

$$\mathcal{F}(\vec{k}_1, \vec{\sigma}_1, \vec{\tau}_1; \vec{k}_2, \vec{\sigma}_2, \vec{\tau}_2) = C_0(f(\vec{k}_1, \vec{k}_2) + f'(\vec{k}_1, \vec{k}_2)(\vec{\tau}_1 \vec{\tau}_2) + g(\vec{k}_1, \vec{k}_2)(\vec{\sigma}_1 \vec{\sigma}_2) + g'(\vec{k}_1, \vec{k}_2)(\vec{\sigma}_1 \vec{\sigma}_2)(\vec{\tau}_1 \vec{\tau}_2)), \quad (1)$$

where $\vec{\sigma}, \vec{\tau}$ are the Pauli matrices in spin and isospin space, respectively; $C_0 = N_0^{-1}$ while $N_0 = p_F m / \pi^2$ is the state density of the one sort particles on the Fermi surface. The single particle momenta \vec{k}_1 and \vec{k}_2 are at the Fermi surface. In the homogeneous medium the functions f, f', g, g' depend on the angle θ between \vec{k}_1 and \vec{k}_2 only. This permits to expand them in Legendre polynomials: $f(\vec{k}_1, \vec{k}_2) = \sum_l f_l P_l(\cos\theta)$ and likewise for f', g, g'

Stability conditions of the ground state with respect to the long-wave excitations were obtained in the paper [1]. The spherical Fermi surface is stable against the small deformations if the parameters in (1) are restricted by certain conditions [1, 4]. Say, for the parameter f_l it is

$$\frac{2f_l}{(2l+1)} > -1. \quad (2)$$

There are analogous expressions for the functions f', g, g' .

In this paper the simple model of interaction (1) is used with the functions $f(\vec{k}_1, \vec{k}_2)$ assumed to be the constants [2, 3]. Hence only the terms with $l = 0$ have nonzero values in the Legendre expansion. Below we omit index 0. In this case the stability criteria are reduced to $f > -1/2$. The same is true for others functions.

The frequencies of the zero-sound collective excitations are the poles of the full scattering amplitude Γ in the matter [2, 4].

$$\Gamma = \mathcal{F} + \mathcal{F}A\Gamma, \quad \Gamma = \frac{\mathcal{F}}{1 - \mathcal{F}A}. \quad (3)$$

Here A is the sum of the two particle-hole loops. One of them corresponds to the excitation of the particle-hole pair and the second one to the absorption. The zero-sound frequency equation

$$1 - \mathcal{F}A(k, \omega, p_F) = 0 \quad (4)$$

can be written for any type of excitations: scalar, spin, isospin, spin-isospin.

In sect.1 we discuss the origin of the ground state instability from the point of view of solutions to (4). It is known [3, 6] that at $f \leq -1/2$ equation (4) has two imaginary solutions. It is shown further how they appear on the physical sheet of the complex plane of ω , where they are at $f > -1/2$. The character of instability related to this solutions is considered. We follow the evolution of the instability while including the pion-nucleon interaction.

Of course at $f \leq -1/2$ we obtain the negative compressibility of matter [2, 3]. This fact and the appearance of the imaginary solutions on the physical sheet are the signals of the phase transition. Thus, there are both the dispersion equation and its imaginary solutions at $f \leq -1/2$. However, there is no the physical object described by them. Nevertheless, the investigation of these solutions can give a useful information about the physical processes in matter.

Equation (4) contains several parameters which characterize the matter. These are the Fermi momentum p_F , the effective nucleon mass m and the constants of the effective interaction (1). We fix the value of p_F and m : $p_F=268$ MeV (this corresponds to the equilibrium density $\rho_0 = 2p_F^3/3\pi^2 = 0.16\text{fm}^{-3}$) and $m = 0.8m_0$, $m_0=0.94$ GeV. The aim of this paper is to investigate the dependence of solutions to the zero-sound equation on the value of f . In the simple model of the quasiparticle interaction the results for the all the types of zero-sound excitations are the same [2, 3].

We demonstrate that there are the various branches of excitations on the physical sheet for the different intervals of the values of f . Namely, 1) at $f > 0$ the zero-sound excitations $\omega_s(k)$ exist, 2) at $-1/2 < f < 0$ solutions are not found, 3) at $f \leq -1/2$ a purely imaginary branch $\omega_P(k)$ of solutions appears. For this branch we find $\omega_P(k)^2 \leq 0$ and $\omega_P(k=0) = 0$. At $-1/2 < f < 0$ $\omega_P(k)$ is placed on the unphysical sheet. The branch $\omega_P(k)$ is responsible for the instability of the ground state with respect to the long-wave excitations.

Let us pass from the zero-sound dispersion equation to pion dispersion equation and consider the waves with quantum numbers $J^\pi = 0^-$. Following Migdal [4, 5], we include the additional interaction corresponding to the one pion exchange into (1)

$$g'_t = g' + \frac{1}{C_0} \left(\frac{f_{\pi NN}}{m_\pi} \right)^2 \frac{k^2}{\omega^2 - m_\pi^2 - k^2}. \quad (5)$$

Replacing g' by g'_t in the expression (1) and using Eq.(5) we obtain after some transforms a pion dispersion equation

$$\omega^2 - m_\pi^2 - k^2 - \Pi(k, \omega, p_F) = 0, \quad (6)$$

$$\Pi(k, \omega, p_F) = - \left(\frac{f_{\pi NN}}{m_\pi} \right)^2 \frac{k^2 A}{1 - C_0 g'_t A}.$$

Here $\Pi(k, \omega, p_F)$ is a pion polarization operator in nuclear matter renormalized by the spin-isospin particle-hole interaction $C_0 g'$.

To simplify the qualitative picture, the isobar-hole intermediate states and scalar part of the polarization operator are not taken into account. But they will be taken into account in several points and this will be indicated specially. The poles of the polarization operator are the solutions to (4). Eq.(6) has the solutions which correspond to $\omega_s(k)$ and $\omega_P(k)$. We denote them by $\omega_s^\pi(k)$, $\omega_P^\pi(k)$. The correspondence is established by the condition that the branches $\omega_s^\pi(k)$ and $\omega_P^\pi(k)$ approach to the poles of polarization operator $\omega_s(k)$ and $\omega_P(k)$ at $f_{\pi NN} \rightarrow 0$.

Our calculations demonstrate that the pion-nucleon interaction distorts the zero-sound branch $\omega_s(k)$ weakly. However the behaviour of $\omega_P(k)$ is changed significantly and we obtain instability of the ground state not only at $g' \leq -1/2$ but also at $g'_p > g' > -1/2$ ($|g'_p| \ll 1$, $g'_p < 0$). At $g'_p > g' > -1/2$ the imaginary branch $\omega_P^\pi(k)$ appears on the physical sheet at the critical density ρ_c at some value of k_c for which $\omega_P^\pi(k_c) = 0$. Momentum k_c is changed from $k \sim p_F$ at $g' \sim 0$ to $k \rightarrow 0$ at $g' \rightarrow -1/2$. At $\rho > \rho_c$ the solutions $\omega_P^\pi(k)$ are on the physical sheet for the certain values momenta. The value of ρ_c is determined by the parameters of matter p_F, m^*, g' .

In sect.2 the solutions to the pion dispersion equation are analyzed. They were regarded in detail in relation to the pion condensation. The results discussed here are complementary to those, obtained in the well-known papers [5, 7]. The pion dispersion equation has the following branches of solution: 1) the pion branch $\omega_\pi(k)$, at $f_{\pi NN} \rightarrow 0$ it is simply $\omega_\pi^2(k) = m_\pi^2 + k^2$; 2) the isobar branch $\omega_\Delta(k)$; 3) the zero-sound $\omega_s^\pi(k)$. Besides there is also 4) 'condensate' branch $\omega_c(k)$ responsible for the pion condensation [8, 9]. It comes from the same point as $\omega_\pi(k)$, $\omega_c(k=0) = m_\pi$ and moves over the unphysical sheet. It goes over to the physical sheet at the density being larger then a critical one $\rho \geq \rho_c$ at certain value of $k = k_1$ and returns to the same unphysical sheet at $k = k_2$. The momenta k_1 and k_2 depend on the density: at the critical density $k_1 = k_2$. On the physical sheet $\omega_c(k)$ is imaginary $\omega_c^2(k) \leq 0$. We see that the behaviour of $\omega_c(k)$ is the same as $\omega_P^\pi(k)$, moreover these branches are on the same unphysical sheet, starting, however, from different points. They come to the physical sheet at different values of g' .

It is shown in sect.3 that for the any value of g' (the values $g' \leq 1$ were considered) there is such a value of the matter density ρ_c that for $\rho \leq \rho_c$ the nuclear matter is unstable. When g' is changed near zero instability with respect to $\omega_P^\pi(k)$ turns into instability with respect to $\omega_c(k)$. This replacement is not apparent on the physical sheet. However this is seen clearly on the unphysical sheet since these branches start in different points: $\omega_P^\pi(k=0) = 0$ and $\omega_c(k=0) = m_\pi$. The interchange of $\omega_P^\pi(k)$ and $\omega_c(k)$ is the result of interaction of the branches on the unphysical sheet: at some $g' = g'_p$ ($|g'_p| \ll 1$, $g'_p < 0$) the branch $\omega_c(k)$ and symmetric $\omega_c^1(k)$ block the branch $\omega_P^\pi(k)$ on the imaginary axis of the unphysical sheet. At $g' < g'_p$ the branch $\omega_P^\pi(k)$ goes to the physical sheet but at $g' > g'_p$ the branch $\omega_c(k)$ does this instead of $\omega_P^\pi(k)$. Thus instability with respect to solutions belonging to the family of solutions responsible for the long-wave instability turns into instability with respect to the pion condensation.

Notice that the equation (6) does not content the information about the structure of the new ground state. It is possible that the pion condensate is present in all cases. The experiments provide $g'_{NN} \sim 1$ [4, 7]. Therefore the instability which is interpreted as the appearance of the pion condensation is related to $\omega_c(k)$ [9].

The problem of the stability of the Fermi liquid with the pion exchange was discussed in papers [10, 11]. There the π - and ρ -meson exchanges were considered as a source for obtaining of the parameters of eq.(1). The meson exchange gives the spin-isospin and tensor contributions into the interaction (1). Stability conditions put the restrictions on the combination of the spin-isospin and tensor terms. However in the Migdal model [4] used here the pion exchange is taken into account in the direct (annihilation) channel only. Whereas the modification of the stability conditions appears due to the tensor terms from the exchange diagrams which are omitted in Migdal model.

In sect.4 the character of the instability related to the $\omega_P(k)$ is investigated. Equation (4) is symmetric with respect to the substitution $\omega \leftrightarrow -\omega$ on the physical sheet. Therefore two branches of solutions differing by the sign emerge simultaneously on the physical sheet. They are on the positive and negative imaginary semiaxis. The both branches point out to the instability of the ground state. If the physical situation is described by solution on the positive semiaxis then the amplitude of the excitation $\omega_P(k)$ is increased as $\sim e^{|\omega_P(k)|t}$. In the opposite case the instability is related to the accumulation of the excitations with zero energy at nonzero momenta $\omega_P(k \neq 0) = 0$. The question is, which of the solutions describe the physical situation.

We suggest the answer to this question for the excitations with the quantum numbers $J^\pi = 0^-$. Following [5] we consider the nuclear matter with one-pion exchange included. There are rules which classify solutions on pertaining to π^+ - or π^- -type [4, 5] in this case. We can obtain an answer by applying these rules to the all solutions of (6) (including $\omega_P^\pi(k)$). The result for the nuclear matter without the inclusion of the pion exchange can be obtained in the limit $f_{\pi NN} \rightarrow 0$. It is shown that the instability of the ground state related to the breaking of the stability conditions (2) appears due to accumulations of the excitations with zero energy $\omega_P(k \neq 0) = 0$.

In paper [12] the pion dispersion equation was study for the relativistic pion propagator. The comparison of our results (here and in [9, 8]) with the results of the paper [12] demonstrates the importance of the relativistic corrections.

1. The instability of the ground state with respect to the long-wave excitations

Let us calculate the particle-hole loop A [4, 7] and put the obtained expression in (4). The dispersion equation for the frequency of the zero-sound is

$$\frac{1}{f} = -4C_0[\Phi(\omega, k) + \Phi(-\omega, k)], \quad (7)$$

where $\Phi(\omega, k)$ stands for excitation of the particle-hole loop and $\Phi(-\omega, k)$ for absorption. For $0 \leq k \leq 2p_F$ the function $\Phi(\omega, k)$ has the form

$$\begin{aligned} \Phi(\omega, k) = & \frac{m}{k} \frac{1}{4\pi^2} \left(\frac{-\omega m + kp_F}{2} - \omega m \ln \left(\frac{\omega m}{\omega m - kp_F + k^2/2} \right) + \right. \\ & \left. + \frac{(kp_F)^2 - (\omega m - k^2/2)^2}{2k^2} \ln \left(\frac{\omega m - kp_F - k^2/2}{\omega m - kp_F + k^2/2} \right) \right). \end{aligned} \quad (8)$$

while, $k > 2p_F$, it reduces to Migdal function

$$\Phi(\omega, k) = \frac{1}{4\pi^2} \frac{m^3}{k^3} \left[\frac{a^2 - b^2}{2} \ln \left(\frac{a+b}{a-b} \right) - ab \right] \quad (9)$$

where $a = \omega - k^2/2m$, $b = kp_F/m$. However, the well-known expression of $\Phi(\omega, k)$ is the Migdal function for all values of k . If substitute the expression (8) into (7) and regroup terms it is easy to express $\Phi(\omega, k)$ as the sum of two Migdal functions. But in this case (7) has two overlapping cuts for $0 \leq k \leq 2p_F$. It is not convenient for us since we study the branches of solutions on the physical and unphysical sheets and the pass from one sheet to another across the logarithmic cuts. Therefore we use (8) for $\Phi(\omega, k)$ at $k \leq 2p_F$ in present paper. Let us consider the cuts of (7). The cuts corresponding to the first and second logarithms in (8) we denote as *I* and *II*. The cuts of the function $\Phi(-\omega, k)$ lie on the negative real semiaxis symmetrically with respect to the cuts of $\Phi(\omega, k)$ (Fig.1). Thus there are four cuts for $k \leq 2p_F$. There are two cuts for $k > 2p_F$. They do not overlap and do not touch the origin of coordinates.

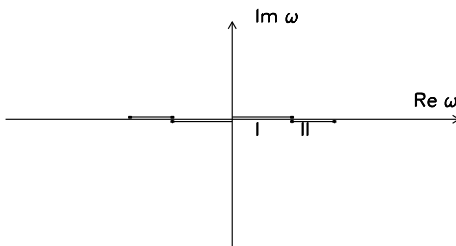


Figure 1: Cuts of eq.(7) in the complex plane of pion frequency.

We note, that for $k/p_F \ll 1$ eq.(7) reduce to the well-known equation for the zero-sound frequency [2, 3]

$$\frac{1}{f} = \frac{s}{2} \ln \frac{s+1}{s-1} - 1$$

with $s = \frac{\omega m}{p_F k}$. Turn now to the analysis of the solutions to (7). First consider zero-sound branches $\omega_s(k)$. We solve Eq.(7) for different values of f both satisfying and not the stability condition (2). The results are shown in Fig.2a ¹. For $f > 0$ the branch $\omega_s(k)$ lies on the real axis of the physical sheet in the interval of momenta $k = (0, k_{fin}^s)$ and has the values ranging from $\omega_s(k=0) = 0$ to $\omega_s(k_{fin}^s) = v_F k_{fin}^s$ ($v_F = p_F/m$ is the velocity of quasiparticles on the Fermi surface [3]).

The branch $\omega_s(k)$ goes over under cut *II* to an unphysical sheet for $k > k_{fin}^s$. The parts of the branches which lie on the unphysical sheet (belonging to the Riemann surface of the second logarithm in (8)) are dashed in Fig.2. Shifting f to the negative values we obtain the solutions disposed in the low semiplane of the same unphysical sheet. In Fig.2a we see that when $\lambda = 1/f$ decreases smoothly from large positive (10^4 , curve 1) to small values ($\lambda = 0.5$ for curve 4 and $\lambda = -0.01$ for curve 5), and then to the large negative values (-10^4 , curve 9) the branches successively transform into one another. The branches $\omega_s(k)$ do not exhibit any singularity that could result in a phase transition.

¹All variables on the figures are given in the pion mass units ($m_\pi=0.14$ GeV). It is naturally for the pion dispersion equation by is convenient for the zero-sound in Fermi liquid also

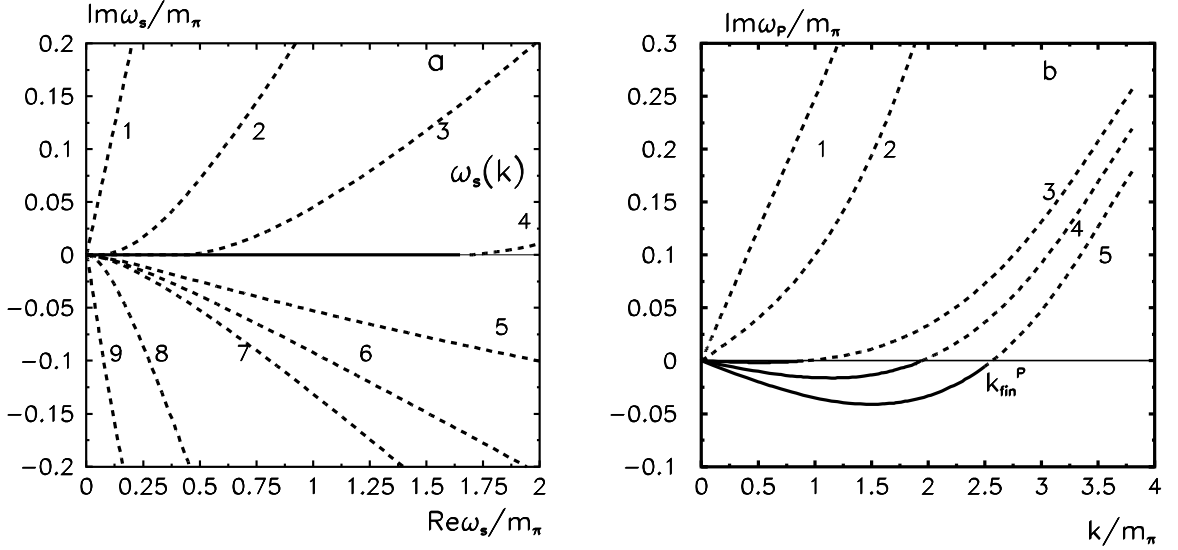


Figure 2: a) Branches $\omega_s(k)$ for the different values of f in the complex plane of ω . The dashed parts of curves lie on the unphysical sheet, $\lambda = 1/f$. The branches are drawn for $\lambda =$ (1) 10^4 , (2) 2.5, (3) 1.0, (4) 0.5, (5) -0.01, (6) -0.5, (7) -1.0, (8) -10.0, (9) -10^4 . b) Branches $\omega_P(k)$ for the different values of f . Branches are presented for $f =$ (1) -0.2, (2) -0.4, (3) -0.51, (4) -0.55, (5) -0.6.

There is, however, yet another set of solutions of (7) which leads to instability of the ground state. We denote it as $\omega_P(k)$. These are pure imaginary solutions. The branches $\omega_P(k)$ lie on the unphysical sheet (belonging to the Riemann surface of the first logarithm in (8)), if the values of the parameters of the effective interaction satisfy Eq.(2). It is shown in Fig.2b that branches $\omega_P(k)$ appear on the negative imaginary semiaxis of the physical sheet for $f \leq -1/2$ at $k = 0$. They terminate under the cut I for $k = k_{fin}^P$. We note that k_{fin}^P increases while $|f|$ increases ($f < 0$). The equation (7) is symmetric with respect to the sign ω and both solutions $\omega_P(k)$ and $-\omega_P(k)$ are on the physical sheet. This illustrates the fact that at $f \leq -1/2$ two imaginary solutions appear [6]. Now consider the influence of the pion-nucleon interaction on $\omega_s(k)$ and $\omega_P(k)$. We search the solutions $\omega_s^\pi(k)$ and $\omega_P^\pi(k)$ to the pion dispersion equation (6) corresponding to $\omega_s(k)$ and $\omega_P(k)$. Polarization operator Π is written in a usual form (without the isobar-hole contribution and scalar part) [13, 8]

$$\Pi = \Pi_N^0/E, \quad E = 1 - \gamma\Pi_N^0/k^2, \quad (10)$$

$$\Pi_N^0(k, \omega) = -4 \left(\frac{f_{\pi NN}}{m_\pi} \right)^2 [\Phi(\omega, k) + \Phi(-\omega, k)]$$

where Φ are given in (8), (9), and $\gamma = C_0 g' \left(\frac{m_\pi}{f_{\pi NN}} \right)^2$. It is easy to see that condition $E = 0$ is the same as Eq.(7). The pion-nucleon vertex contains form factor of pion $d(k^2) = (\Lambda^2 - m_\pi^2)/(\Lambda^2 + k^2)$ ($\Lambda = 0.667$ GeV).

Consider the branches $\omega_P^\pi(k)$. In Fig.3a we show the changing of the branches $\omega_P^\pi(k)$ with increasing $f_{\pi NN}$. The curve 1 is the same as the curve 2 in Fig.2b which is $\omega_P(k)$ for $g' = -0.4$. The behaviour of $\omega_P^\pi(k)$ is changed drastically from the physical point of view, when $f_{\pi NN}$ increases. For

the experimental value $f_{\pi NN} = 1$ the imaginary $\omega_P^\pi(k)$ goes over to the physical sheet in interval of the values of momenta (k_1, k_2) . This signals the presence of instability. It is seen that k_1, k_2 are not small in comparison with p_F and the springing up instability is not the long-wave one.

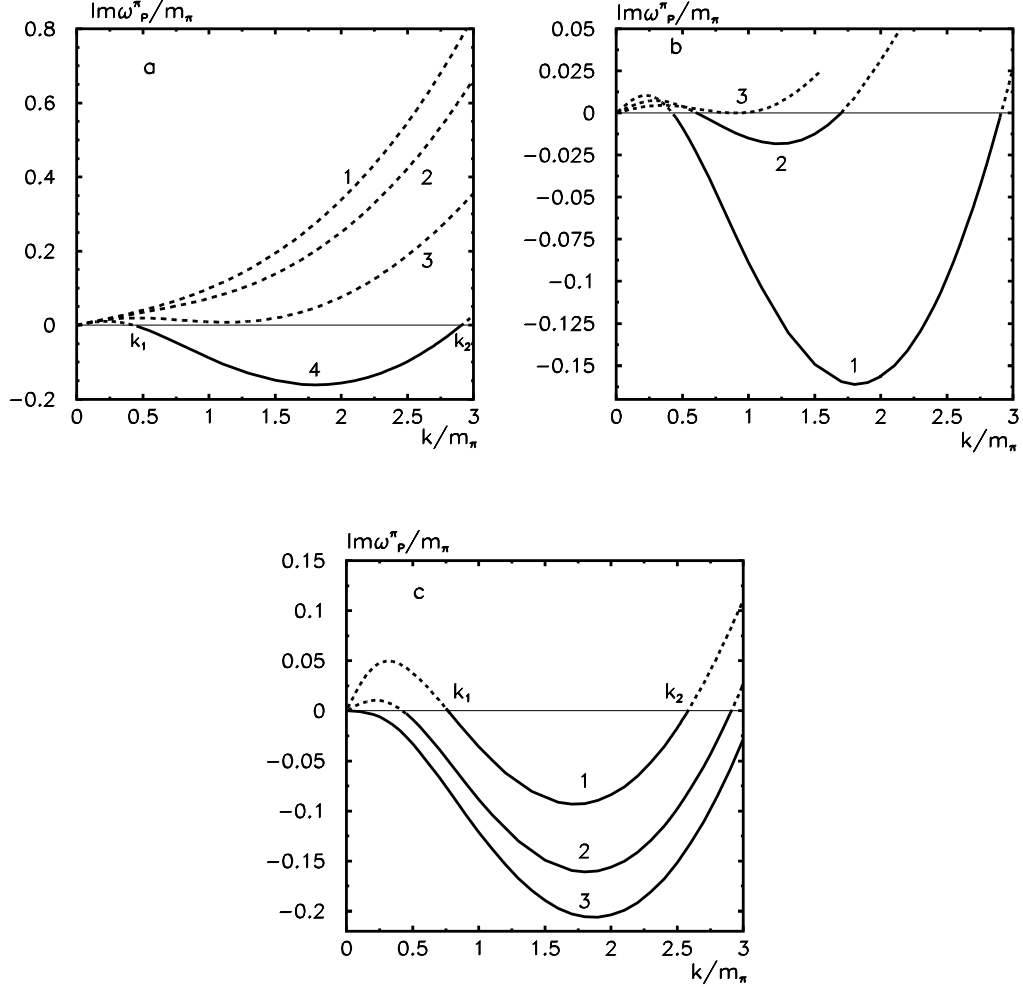


Figure 3: The branches $\omega_P^\pi(k)$. The dashed parts of curves lie on the unphysical sheet. a) Dependence on pion-nucleon coupling constant is presented at $g' = -0.4$ and $\rho = \rho_0$ for: $f_{\pi NN} =$ (1) 0.0, (2) 0.3, (3) 0.6, (4) 1.0. b) Dependence on the nuclear matter density at $g' = -0.4$ and $f_{\pi NN}=1.0$ for: $\rho/\rho_0 =$ (1) 1.0, (2) 0.1. c) Dependence on the value of g' at $\rho = \rho_0$ and $f_{\pi NN}=1.0$ for: $g' =$ (1) -0.2, (2) -0.4, (3) -0.55.

The dependence of the instability on matter density is demonstrated in Fig.3b. Curve 1 coincides with the curve 4 of Fig.3a and it is calculated for the equilibrium density ρ_0 . Curve 2 is presented for the density $0.1\rho_0$. The critical density for the parameters $f_{\pi NN} = 1$, $g' = -0.4$ is equal to $\rho_c = 0.07\rho_0$. For $\rho < \rho_c$ the nuclear matter is stable (curve 3). In Fig.3c the branches of solutions $\omega_P^\pi(k)$ for different g' are presented. We can see how the condition (2) is realized by $\omega_P^\pi(k)$. For g' larger then the critical one: $0 > g' > -1/2$, the interval of the values of the momenta $k_1 \leq k \leq k_2$ for which the solution is on the physical sheet decreases with decreasing of the density (Fig.3b). The

instability disappears for $\rho < \rho_c$. However, for $g' \leq -1/2$ the instability exists at any density. This is clear because the branches $\omega_P(k)$ and $\omega_P^\pi(k)$ are close one to another at small k because of the weakness of the pion-nucleon interaction (5) and condition (2) does not depends on density.

2. The instability of the ground state with respect to the pion condensation

As it was shown by Migdal [5] the pion dispersion equation (6) has the solutions with negative frequency squared. Such solutions emerge if the density becomes larger that some critical one. This observation became the starting point of development of pion condensation theory.

In Fig.4 [9] it is shown the behaviour of pion dispersion solutions in the complex plane of a pion frequency. The solutions are presented for the pion dispersion equation with inclusion of isobar-hole excitations and the scalar part of polarization operator Π_s [8]. The values of parameters are $g'_{NN} = 1.0$, $g'_{\pi\Delta} = 0.2$, $g'_{\Delta\Delta} = 0.8$. In Fig.4 the branches of solutions are presented for nonzero isobar width $\Gamma_\Delta = 115$ MeV. Owing to the width it is easier to trace the behaviour of the branches as functions of k . When $\Gamma_\Delta = 0$ the branches ω_π , ω_s^π and ω_Δ become real and ω_c pure imaginary ($\text{Im } \omega_c(k) \leq 0$) (Fig.4) on the physical sheet. It is ω_c that has the negative frequency squared. The critical density in these calculations is $\rho_c \simeq 1.2\rho_0$, this correspond to Fermi momentum $p_{Fc} = 283$ MeV. In Fig.4 the solutions are presented for the values of Fermi momenta which are a little smaller than p_{Fc} , i.e. $p_F = 268$ MeV (corresponding to equilibrium density) and a little larger than p_{Fc} , i.e. $p_F = 290$ MeV. The latter case demonstrates the appearance of $\omega_c(k)$ on the physical sheet).

In Fig.4a the zero-sound branch $\omega_s^\pi(k)$ is shown. It begins at the point $\omega_s^\pi(k = 0) = 0$, moves along the real axis and goes over under the cut II at k_{fin}^s . In Fig.4b the isobar branch $\omega_\Delta(k)$ is shown, it issues from the point $\omega_\Delta(k = 0) = m_\Delta - m_N$ and terminates under the cut of the isobar polarization operator [8]. In Fig.4c the pion branch $\omega_\pi(k)$ is presented, $\omega_\pi(k = 0) = m_\pi^*$, $m_\pi^{*2} = m_\pi^2 + \Pi_s$. It terminates under the isobar cut as well. In Fig.4d the relative placement of $\omega_\pi(k)$ and $\omega_c(k)$ is presented. The branch $\omega_c(k)$ appears on the physical sheet and returns on the same unphysical sheet under the cut I .

The dependence of $\omega_c(k)$ on the isobar width and nuclear density is demonstrated in Fig.5. In Fig.5a the behaviour of $\omega_c(k)$ at $\Gamma_\Delta \rightarrow 0$ is shown. The curve 1 corresponding to $\Gamma_\Delta = 0$ shows that the solutions on the physical sheet are pure imaginary. In Fig.5b we show the dependence of $\omega_c(k)$ on density. When the Fermi momentum is less than the critical one $p_F < p_{Fc}$ the branch does not appear on the physical sheet (curve 1) and lies on the unphysical sheet completely.

For the further analysis of the interaction of branches $\omega_c(k)$ and $\omega_P(k)$ we need more detailed picture of the behaviour of the solutions on the unphysical sheet. In Fig.6 we use the same model as in Figs.4,5 with $\Gamma_\Delta = 0$ [8]. The parts of branches which lie on the imaginary axis are shifted in different sides to demonstrate the change of branches with k . In Fig.6 a new branch $\omega_c^1(k)$ is presented besides $\omega_c(k)$. It does not appear on the physical sheet but it is the third ingredient of the interaction of $\omega_c(k)$ and $\omega_P^\pi(k)$. We see that the branch $\omega_c(k)$ and symmetric branch $\omega_c^1(k)$ coincide in the imaginary axis (at $k_A = 1.09m_\pi$) on the unphysical sheet in point A . At larger k the branch

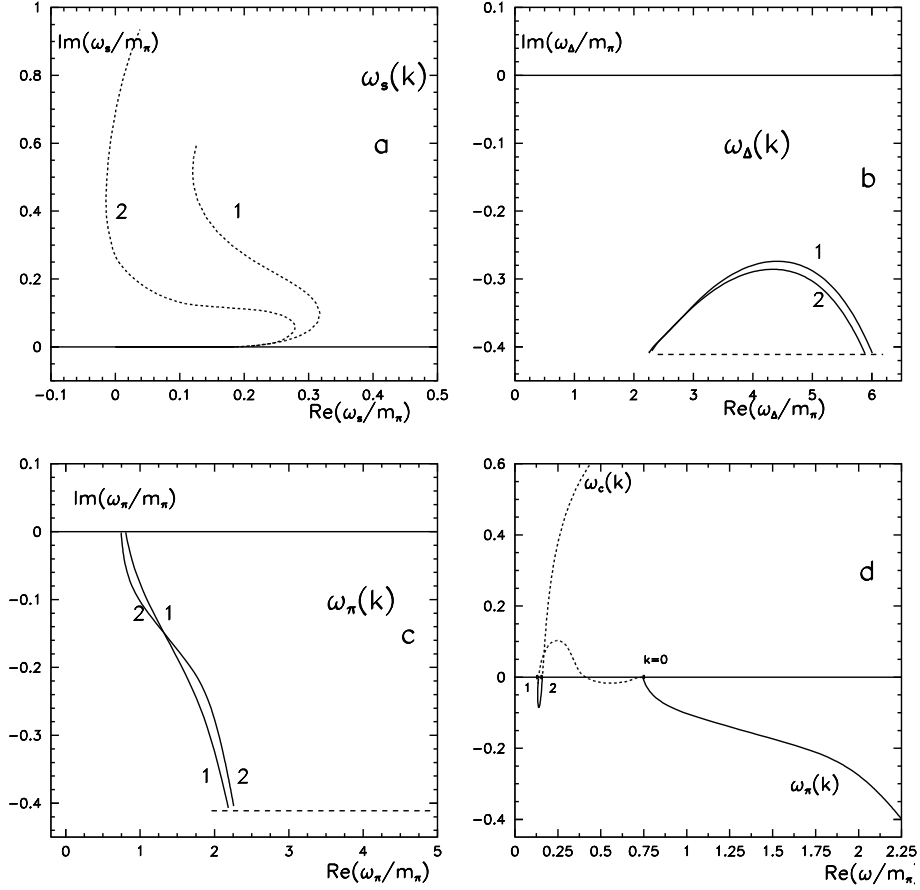


Figure 4: Branches of solutions to Eq.(6) in the complex plane of ω : a) zero-sound wave $\omega_s^\pi(k)$, b) isobar branch $\omega_\Delta(k)$ [the horizontal dashed line depicts the cut of isobar polarization operator [9] at $p_F = 290$ MeV for the momentum value at which $\omega_\Delta(k)$ goes under the cut], c) pion branch $\omega_\pi(k)$ [the horizontal dashed line has the same meaning as in Fig.(b)], d) the branches $\omega_\pi(k)$ and $\omega_c(k)$ at $p_F=290$ MeV. The curves 1 (2) corresponds to $p_F= 268$ (290) MeV. The dashed parts of curves lie on the unphysical sheet.

$\omega_c(k)$ goes down along the imaginary axis and goes over to the physical sheet. The branch $\omega_c^1(k)$ goes up. At $k \simeq 1.8m_\pi$ the branches turn back and meet one another again in the point B ($k_B = 3.08m_\pi$) then they pass in the opposite sides on the unphysical sheet of complex plane. Fig.6 clarifies the behaviour of the curve 1 in Fig.5a when function sharply changes the dependence on k in two points. The branch $\omega_c(k)$ is pure imaginary when the value of k changes in the interval between k_A and k_B .

Note that at the critical density ρ_c the branch $\omega_c(k)$ appears on the physical sheet at the only point $k = k_c$. At this point $\omega_c^2(k_c) = 0$. This solution is a signal that the phase transition in nuclear matter takes place [4]. The solutions at larger densities are not related to a real physical object. Nevertheless, it is very useful to consider the solutions at $\rho \geq \rho_c$.

3. Interaction of branches $\omega_P^\pi(k)$ and $\omega_c(k)$

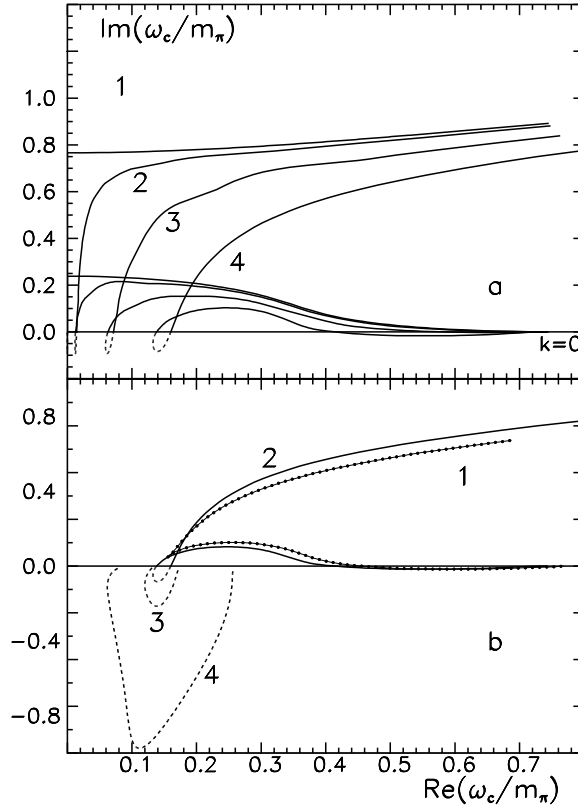


Figure 5: Condensate branch ω_c in the complex plane of ω [the dashed (solid) curves represent those parts of the solutions branches that lie on the physical (unphysical) sheets]: a) branch $\omega_c(k)$ at $p_F=290$ MeV for isobar-width values of $\Gamma_\Delta = (1) 0, (2) 10, (3) 50$ and $(4) 115$ MeV; b) branch $\omega_c(k)$ at $\Gamma_\Delta = 115$ MeV for Fermi momentum values of $p_F = (1) 280, (2) 290, (3) 300$ and $(4) 360$ MeV. Only the solutions on the physical sheet are displayed for the curves 3 and 4. Curve 1 for $p_F=280$ MeV completely lies on unphysical sheet.

Let us consider the solutions to the pion dispersion equation on the physical sheet for g' near zero $g' = (-0.05, 0.05)$. [Now we return to the version of calculation without the isobar and scalar part of polarization operator ($m_\pi^* = m_\pi$).] In Fig.7 we show how the branches change with g' . The branches $\omega_c(k)$ is shown by dashed curves while $\omega_P^\pi(k)$ is presented by the solid line. Recall that the branches go over to the physical sheet across the cut I . Looking at Fig.7a we can not notice the transition from one type of instability to another. But this transition becomes visible if we turn to Fig.7b, where the same results are presented in the larger interval of momenta. The curves 4, 5 start at the point $\omega = 0$ at $k = 0$ whereas curves 1, 2, 3 are drawn from the momentum $k = k_A$ only, since they are complex at $k < k_A$ (compare with Fig.6 made in the complex plane). They behave themselves as $\omega_c(k)$ in Fig.6, starting from $\omega = m_\pi$ at $k = 0$.

As mentioned above the appearance of $\omega_P^\pi(k)$ or $\omega_c(k)$ on the physical sheet takes place at the density larger the critical $\rho \geq \rho_c$ at $g' > -1/2$. The value ρ_c is determined by parameters of matter: $m, g', f_{\pi NN}$.

We can not determine, if the replacement of the branches took place if we limit ourselves to the

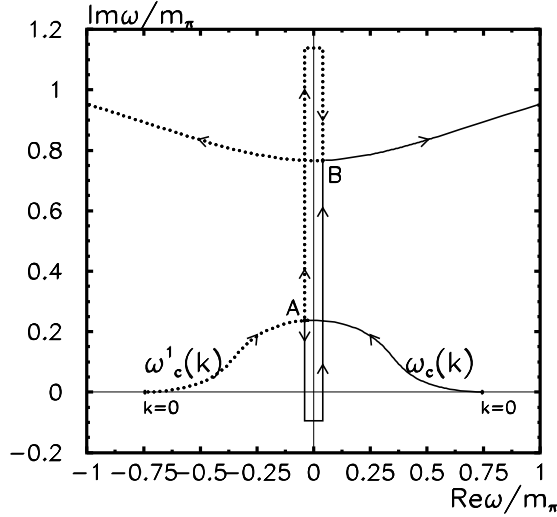


Figure 6: Branches $\omega_c(k)$ and $\omega_c^1(k)$ in the complex plane of ω , $p_F = 290$ MeV. The part of the complex plane above the x-coordinate axis is the unphysical sheet and the semiplane below the x-axis is a physical sheet. The arrows show the direction of increasing of the momentum k along the branches.

physical sheet only. This is illustrated in Fig.8. Here the dependence of the critical Fermi momenta p_{Fc} on g' is demonstrated (i.e. the values of p_F for which (6) has solutions $\omega = 0$ for different g' at the momenta $k = k_c$). Looking at the curve we cannot say that the instability with respect to $\omega_P(k)$ is changed by the instability with respect to $\omega_c(k)$. However the investigations similar to those, demonstrated in Fig.7, show that the replacement takes place at $g' = -0.0009$. The dependence of k_c on g' (dashed curve) demonstrates how the instability becomes the long-wave one if $g' \rightarrow -1/2$.

A mechanism of the replacement of branches is presented in Fig.9. We show three interacting branches: $\omega_c(k)$, $\omega_c^1(k)$ and $\omega_P(k)$ at values g' near g'_p in the complex plane of ω . In the present calculation we have $-0.00102 < g'_p < -0.001$. In Fig.9a at $g' = -0.00102$ the branch $\omega_P^\pi(k)$ moves between $\omega_c(k)$ and $\omega_c^1(k)$: $k_3 = 0.08m_\pi$, and $k_2 = 0.091m_\pi$. At $k > k_3$ $\omega_P^\pi(k)$ goes down and penetrates to the physical sheet (we can compare with Fig.3). The minimal value of $\omega_P^\pi(k)$ is reached at $k_{min} = 1.65m_\pi$.

In Fig.9b at $g' = -0.001$ the branches $\omega_c(k)$ and $\omega_c^1(k)$ blockade $\omega_P^\pi(k)$. The branches $\omega_c(k)$ and $\omega_c^1(k)$ meet in the point A on the imaginary axis ($k_A = 0.09238m_\pi$). The branch $\omega_c^1(k)$ goes up and meets the branch $\omega_P^\pi(k)$ at $k = 0.09242m_\pi$. After that these branches go to the opposite sides on the complex plane. But at $k > k_A$ the branch $\omega_c(k)$ goes down to the physical sheet, as it was discussed in Fig.6 in detail.

Thus, there is a replacement of branches which go over to physical sheet and responsible for the instability of the ground state. The branch $\omega_P^\pi(k)$ is changed by $\omega_c(k)$. It was explained in the previous section that $\omega_P^\pi(k)$ belongs to the family of solutions, which gives the long-wave instability at $k \rightarrow 0$ and $g' \rightarrow -1/2$. On the other side, the instability related to $\omega_c(k)$ is interpreted as appearance of the pion condensation.

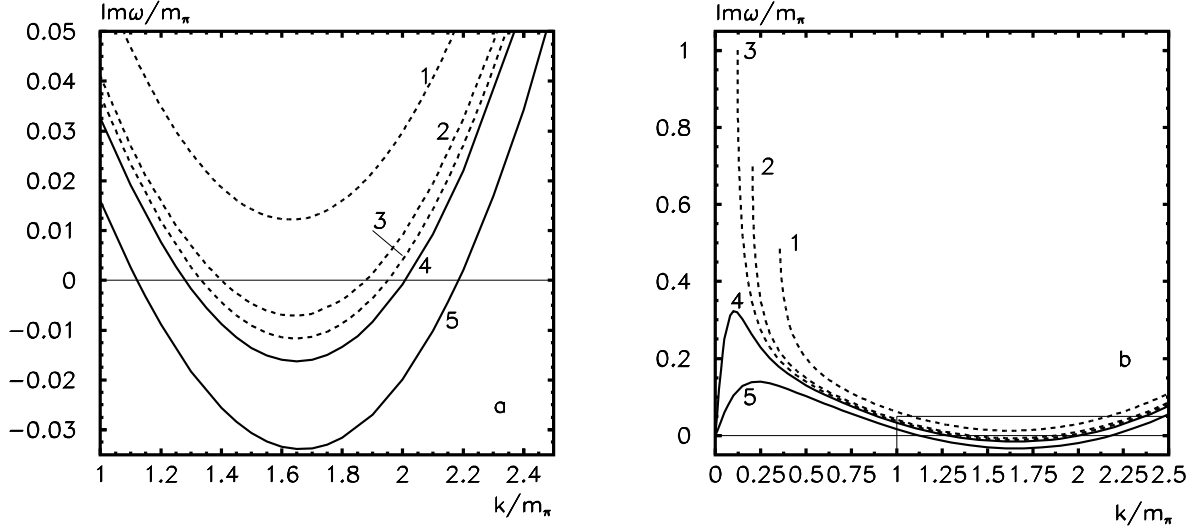


Figure 7: Imaginary solutions of (8) for $g' = (1) 0.05, (2) 0.01, (3) 0.0, (4) -0.01, (5) -0.05$. The part of the complex plane above the x-coordinate axis is the unphysical sheet and the semiplane below the x-axis is a physical sheet. The solid (dashed) curves correspond to $\omega_P(k)$ ($\omega_c(k)$). a) The interval of momentum values $k/m_\pi = (1.0, 2.5)$; b) the interval of momentum values $k/m_\pi = (0.0, 2.5)$. The rectangle on the right below is the figure a).

4. Investigation of the character of instability of the ground state related to $\omega_P(k)$ and $\omega_P^\pi(k)$

The existence of the solution of the dispersion equation with $\omega_i^2(k) \leq 0$ on the physical sheet of the complex plane of ω demonstrate the instability of the ground state. The equations (6), (7), (10) are symmetric with respect to the sign of ω on the physical sheet, therefore we have two solutions differing by sign. In Figs.2b,3,6,7 there are presented solutions which are placed on the negative imaginary semiaxis on the physical sheet. Besides there are solutions on the positive semiaxis.

In this section we investigate which of solution describes the instability of the ground state. Turn to the pion dispersion equation (6). The following selection rules for physical solutions has been formulated by Migdal [14]. The rules sort the solutions on relating to π^+ - or π^- -type [4, 5]. All solutions with

$$\frac{d}{d\omega}(\omega^2 - m_\pi^2 - k^2 - \Pi) > 0 \quad (11)$$

at $\omega = \omega_i(k)$, correspond to π^+ -meson type, while those with

$$\frac{d}{d\omega}(\omega^2 - m_\pi^2 - k^2 - \Pi) < 0 \quad (12)$$

at $\omega = \omega_i(k)$ after the substitution $\omega = -\omega_i(k)$ give the π^- -meson dispersion relation. For π^+ type excitation we compare the values $\varepsilon_k = \omega_i(k)$ with the physical energies while for π^- type we compare the values with the opposite sign $\varepsilon_k = -\omega_i(k)$ with the physical energies. These rules are written for the real solutions $\omega_i(k)$ and we cannot apply them to $\omega_P^\pi(k)$ presented above.

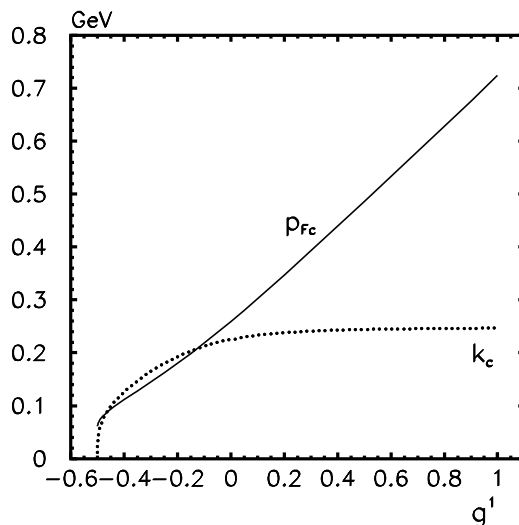


Figure 8: Dependence of the critical Fermi momentum p_{Fc} on g' (solid line). Dependence of k_c on g' (dashed line).

However, the behaviour of $\omega_P^\pi(k)$ and $\omega_P(k)$ is changed if we take a large $|g'|$ ($g' < 0$). In Fig.10a the branch $\omega_P(k)$ at $g' = -2$ is presented. We see that at the large negative values of g' (or f, f', g) part of branch lies on the real axis. The explanation is the following. In Fig.2b we have seen that the value of k_{fin}^P increases simultaneously with $|g'|$. The momentum k_{fin}^P denotes the final momentum when the branch leaves the physical sheet. It occurs that at $g' \simeq -2$ the value $k_{fin}^P > 2p_F$. It was mentioned above that the cuts of the polarization operator at $k > 2p_F$ do not touch the origin of coordinates. Thus, the branch $\omega_P(k)$ (Fig.10a) returns to the origin of coordinates along the imaginary axis having the momentum $k_{int} > 2p_F$ (point 2), but there is no the cut. As it is shown in Fig.10a the branch turns to the real axis at $k > k_{int}$. While k increases, this branch penetrates through the cut (at $k = k_{fin}^P$, point 3) and goes to the unphysical sheet under the cut. In some interval of momenta there is a real solution. In Fig.10b the analogous picture for $\omega_P^\pi(k)$ is presented (curve 1, $g' = -3$). The calculations in Fig.10b are carried out with isobar-hole excitations and the scalar part of the polarization operator being taken into account [8].

Now we apply the rule (11) to the part of $\omega_P^\pi(k)$ which is purely real (curve 1, Fig.10b) and obtain that this part of branch belongs to π^+ -type. But we cannot find whether the continuation of the real part to smaller $k < k_{int}$ lies on the positive or negative imaginary semiaxis. This may be checked easily including isobar width into consideration. The curves 2 and 3 in Fig.10b correspond to $\Gamma_\Delta = 50$ and 100 MeV. At $\Gamma_\Delta \rightarrow 0$, the curves approach the curve 1.

Now we can draw a conclusion that curve 1 (Fig.10b) lying on the negative imaginary semiaxis at $k < k_{int}$ belongs to π^+ -type excitations. This conclusion is the only information we need. Considering the pion dispersion equation at large $|g'|$ ($g' < 0$) we remember that there is a phase transition at $g' \leq -1/2$ at the any density. Then, the values of k are too large for the simple model of zero-sound. But it was demonstrated above that there is a continuous passage on g' and k to the range of values where the Fermi liquid theory is valid.

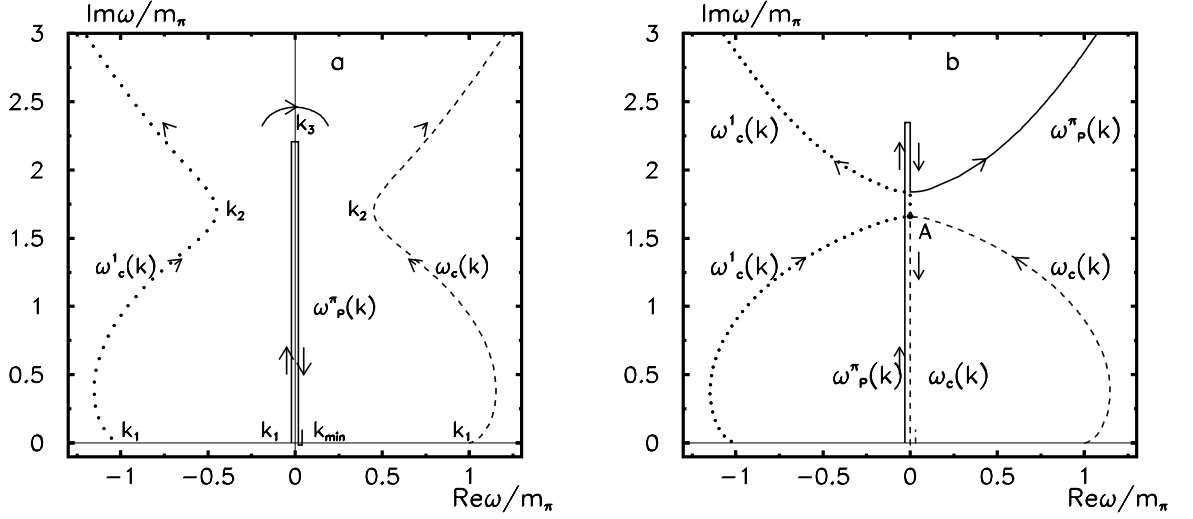


Figure 9: Interaction of the branches $\omega_P(k)$ (solid), $\omega_c(k)$ (dashed) and $\omega'_c(k)$ (dotted): a) $g' = -0.00102$, $k_2/m_\pi = 0.091$, $k_3/m_\pi = 0.08$, $k_{min}/m_\pi = 1.65$; $\omega_P(k)$ goes over to the physical sheet, b) $g' = -0.001$, $k_A/m_\pi = 0.09238$; $\omega_c(k)$ goes over to the physical sheet. The part of the complex plane of ω above the x-coordinate axis is the unphysical sheet, below the x-axis is a physical sheet. Momentum $k_1 = 0$. The arrows show the direction of increasing of the momentum k along the branches.

In correspondence with (11) the physical energies which determine the character of the instability are $\varepsilon_k = \omega_P(k) = -i|\omega_P(k)|$. It means that the instability emerges due to accumulation of the excitations with zero energy in the ground state but not because of the exponential increasing of solution amplitudes.

As it is shown in Fig.3a (and can be easily seen from (6)) there is a continuous passage from $\omega_P^\pi(k)$ to $\omega_P(k)$ when $f_{\pi NN} \rightarrow 0$. Therefore the conclusion about the character of instability remains true for $J^\pi = 0^-$ wave for the nuclear matter without pion-nucleon interaction taking into account as well.

Summary

In this paper the solutions to the zero-sound frequency equation and pion dispersion equation are considered as the functions of parameters of the effective quasiparticle interaction values (1).

1) We obtained the imaginary solutions ($\omega_P(k)$) to the zero-sound frequency equation (7) responsible for the instability of the ground state with respect to the long wave excitations. The branches $\omega_P(k)$ are obtained for the different values of constants $f < 0$ of the effective quasiparticle interactions. These branches lie on the unphysical sheet when f satisfy the stability conditions (2). However if $f \leq -1/2$, the imaginary branches $\omega_P(k)$ go over to the physical sheet of the complex frequency plane in some interval of momenta (k_1, k_2). The value of k_2 depends on f , p_F , m^* while $k_1 = 0$. This is a signal about the instability of the ground state with respect to the long-wave excitations.

2) The solution branches of $\omega_P^\pi(k)$ corresponding to $\omega_P(k)$ are obtained for the pion dispersion

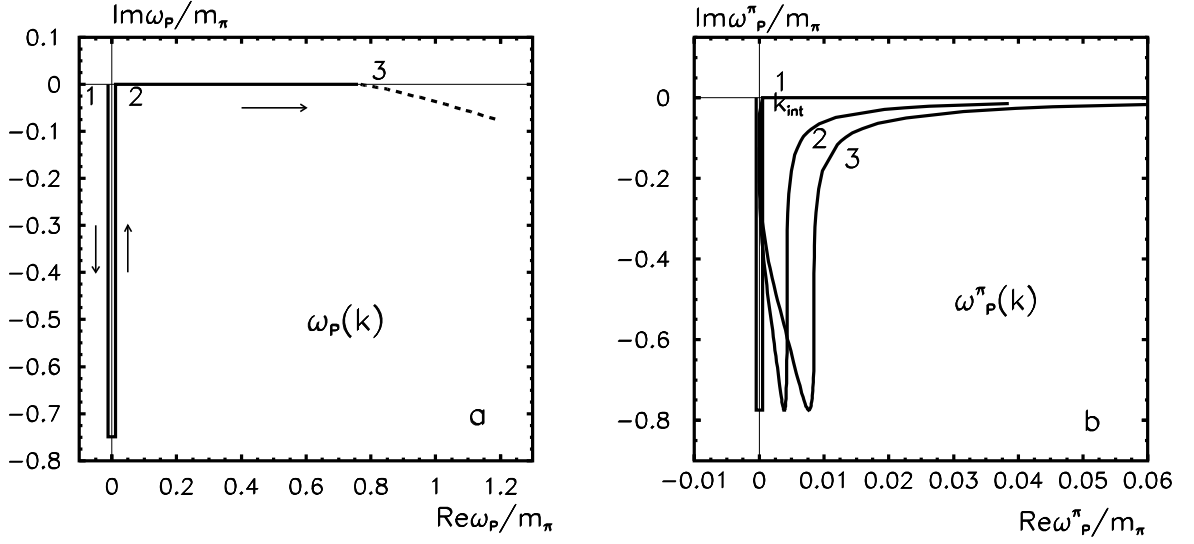


Figure 10: a) The branch $\omega_P(k)$ at $g' = -2.0$ on the physical sheet of the complex plane of ω . The beginning of branch (point 1): $k_1=0$; branch turns from imaginary to real meanings in (2): $k_2/m_\pi = k_{int}=4.8$; it terminates under the cut (3) $k_3/m_\pi = k_{fin}^P=5.4$. b) The branch $\omega_P^\pi(k)$ at $g'=-3.0$. The full pion polarization operator [8, 9] is used. The dependence of $\omega_P^\pi(k)$ on isobar-width $\Gamma_\Delta = (1) 0, (2) 50, (3) 100$ MeV.

equation (6). It is shown that the branches $\omega_P^\pi(k)$ pass to $\omega_P(k)$ if $f_{\pi NN} \rightarrow 0$. The solutions $\omega_P^\pi(k)$ give instability at all negative values of g' . When $g' \leq -1/2$ the instability emerges at any density in correspondence of (2). At $-1/2 < g' < 0$ nuclear matter becomes unstable at some density larger the critical one: $\rho > \rho_c$. The value of density ρ_c depends on g' and other parameters of the theory.

3)The four branches of solutions to the pion dispersion equation (6) with quantum numbers $J^\pi = 0^-$ are obtained [9]. Besides the well-known solutions: zero-sound, pion and isobar, the fourth branch $\omega_c(k)$ responsible for the pion condensation is presented.

4)It is shown how the instability of the ground state with respect to $\omega_P^\pi(k)$ is replaced by the instability with respect to $\omega_c(k)$ when g' changes near zero. We cannot distinguish are the branches of solutions $\omega_P^\pi(k)$ or $\omega_c(k)$ at $g' < 0$ on the physical sheet. However these branches are simply identified on the unphysical sheet since they issue from different points: $\omega_P^\pi(k=0) = 0$ and $\omega_c(k=0) = m_\pi$. At small k they are on the unphysical sheet. It is shown that at $g' = g'_p$ the part of $\omega_P^\pi(k)$ which is placed on the physical sheet is replaced by the part of $\omega_c(k)$. This replacement is the result of the interaction of three branches $\omega_P^\pi(k)$, $\omega_c(k)$ and $\omega_c^1(k)$ on the unphysical sheet. Instability with respect to the solution belonging to the family responsible for the long-wave instability is changed by instability with respect to the "pion condensation".

5)The character of instability of the ground state with respect to the long-wave excitations is considered. The zero-sound frequency equation (7) and the pion dispersion equation (6) are symmetric with respect to the transformation $\omega \leftrightarrow -\omega$. Therefore at $f \leq -1/2$ the two imaginary solutions: $\omega_P(k)$ and $-\omega_P(k)$ appear on the physical sheet. The both of them point out that the phase transition took place. Applying the Migdal's selection rules to $\omega_P^\pi(k)$ for the case of the large negative

g' , we observe that $\omega_p^\pi(k)$ which is lying on the negative imaginary semiaxis belongs to π^+ -type excitations. This means that the corresponding energies of physical excitations have the negative imaginary parts. Then the ground state is unstable due to accumulation of zero energy excitations in the ground state, but not because of the exponential increasing of the any solution amplitudes.

The author is grateful to E.E.Saperstein for setting up a problem of the stability conditions and M.G.Ryskin and E.G.Drukarev for stimulating discussion.

This work was supported by the Russian Foundation for Basic Research (project no.00-02-16853), DFG (project 438/RUS 113/595/0-1).

References

- [1] Pomeranchuk I.Ya., Sov.Phys. JETP **8** (1958) 361.
- [2] Lifshits E.M., Pitaevsky L.P., *Theoretical Physics X* (Nauka, Moscow,1979).
- [3] Pines D., Nozieres P., *The Theory of Quantum Liquids* (Benjamin, NY,1966).
- [4] Migdal A.B., *Theory of the Finite Fermi Systems and Applications to Atomic Nuclei* (Nauka, Moscow, 1983).
- [5] Migdal A.B., Rev.Mod.Phys.**50** (1978) 107; Migdal A.B., Voskresensky, Saperstein E.E. and Troitsky M.A., *Pionic Degrees of Freedom of Nuclear Matter* (Nauka, Moscow,1991); Phys.Rep.**192** (1990) 179.
- [6] Thouless D.J., *The Quantum Mechanics of Many-Body Systems* (Academic Press, NY,1972).
- [7] Ericson T., Weise W., *Pions and Nuclei*, (Clarendon Press,Oxford, 1988).
- [8] Drukarev E.G., Ryskin M.G., Sadovnikova V.A., Eur.Phys.J. **A4** (1999) 171.
- [9] Sadovnikova V.A., Ryskin M.G., Phys. of Atom.Nucl. **64** (2001)440, V.A.Sadovnikova, nucl-th/0002025.
- [10] Backman S.-O., Sjoberg O., Jackson D.D., Nucl.Phys. **A321** (1979) 10.
- [11] Brown G.E., Backman S.-O., Oset E. and Weise W. Nucl.Phys. **A286** (1977) 191.
- [12] L.-G. Liu, Masahiro Nakano, Nucl.Phys. **A618** (1997) 337.
- [13] W.H.Dichkoff, A.Faessler, J.Meyr-ter-Vehn, and H.Muther, Phys.Rev. **C23** (1981) 1154.
- [14] Migdal A.B., Phys.Rev.Lett. **31** (1973) 257.